

Binding site of amiloride to urokinase plasminogen activator depends on species

JERZY JANKUN¹⁻⁴ AND EWA SKRZYPCZAK-JANKUN^{1,4}.

¹Urology Research Center, ²Department of Urology, ³Physiology and Molecular Medicine, Medical College of Ohio, Toledo, OH 43614-5807; ⁴Department of Chemistry, The University of Toledo, Toledo, OH 43606-3390, USA

Abstract. Novel drug candidate is checked on its potency on animal models before it can advance to human phase of the research. Usually negative results on animal phase disqualify it. Targeting specific enzymes by small chemicals rises the question about appropriateness of this approach. As an example, the urokinase (uPA) is recognized as an important enzyme responsible for cancer metastasis and angiogenesis. It is therefore important to ask the question if small chemical will inhibit uPA of different species with the same or different potency. Using DNA sequence and known structure of uPA we have modeled 3D structures of uPAs for several different species. By theoretical calculations we have determined most probable structure of amiloride/uPAs complexes. Catalytic triad (B57, B102, B195) and specificity pocket (B187-B197, B212-B229) are highly conserved in all cases, and are the regions responsible for proteolytic activity and recognition of the substrate. Significant differences were observed in a different region (loop B93-B101), that we identified as binding site of amiloride to the tissue plasminogen activator (tPA). Although tPA shares the same function of activating plasminogen and it is structurally similar to uPA. Amiloride is a specific inhibitor of uPA but does not inhibit tPA. Our study shows that predicted position of amiloride depends on species and in some cases was located, as expected, in the specificity pocket, but in the other cases close to the loop B93-B101. This location could weaken affinity of binding or prevent inhibition of uPA at all. Therefore, drug screening and elimination process based solely on animal study, without careful structural analysis, could lead to the elimination of potential drug for humans.

Introduction

Uncontrollable spread of tumors caused by cancer metastasis is responsible for most of cancer-related death. The proteolytic degradation of the extracellular matrix (ECM) is recognized as a mechanism that plays an important role in the metastatic process. Proteolytic enzymes are required to mediate tumor cell invasion to adjacent tissues and initiate the metastatic process. The urokinase plasminogen activator system (uPAs) is commonly overexpressed by many different human cancers (1). An increased amount or activity of uPA, or urokinase plasminogen activator receptor (uPAR) has been found in human cancer cell lines with metastatic behavior (2-4). Moreover, animals injected with cancer cells expressing higher amounts of uPA and/or uPAR develop metastatic lesions earlier and more frequently than animals injected with the same cell expressing lower amounts of uPA/uPAR (5). Additionally, it has been reported that uPA activity is increased in metastatic tumors compared with primary tumors in experimental animals (6). The other plasminogen activator - tissue type plasminogen activator (tPA) is rarely overexpressed in malignant tumors and does not seem to be relevant in the metastatic process but is important in blood clotting processes (3, 7).

The uPA system contains the following elements: (i) *Plasminogen* - an enzyme that in its inactive form is called plasminogen, and in active form called plasmin. Plasmin is a strong proteolytic enzyme able to digest proteins of connective tissue and basement membranes. It is also able to activate other latent proteolytic enzymes, broadening the spectrum of proteins attacked. Pro-collagenase is activated to collagenase in this manner. Plasmin is a key enzyme in the mechanism responsible for tissue remodeling, tumor invasion and development of distant metastasis. (ii) *Activators* - uPA and tPA. Both are weak proteolytic enzymes that activate plasminogen to plasmin by proteolytic cleavage. uPA is involved in pericellular proteolysis during cell migration, wound healing, and tissue remodeling under variety of physiological and pathological conditions. tPA mainly mediates intravascular thrombolysis (3, 8). (iii) *Inhibitors of plasminogen activators*. There are four known inhibitors of uPA: PAI-1, PAI-2, PAI-3 and a protein called nexin. All of them are regulatory proteins mediating proteolysis on the activation level. Most relevant in the metastatic process is PAI-1, which exists in three different forms:

Correspondence to: Dr. Jerzy Jankun, Urology Research Center, Medical College of Ohio, Toledo, OH 43614-5807,
E-mail: jerzy@golemxiv.dh.mco.edu,
or to: Dr. Ewa Skrzypczak-Jankun, Chemistry Department, The University of Toledo, 2801 W.Bancroft St., Toledo OH 43606-3390,
E-mail: ejankun@protein.wo.utoledo.edu.

Key Words: urokinase, amiloride, binding site, cancer, human, baboon, chicken, mouse, rat, chicken.

inactive-latent, cleaved, and active form. (iv) *uPA receptor* (uPAR). The binding site of uPA is called the uPA receptor. It is a glycoprotein that binds uPA to the cell surface. While uPA retains its ability to activate the plasminogen. High numbers of uPA receptors on the surface of cancer cells, if occupied by uPA, create high proteolytic activity in the proximity of cancer cells (9).

All serine proteases (uPA and tPA are members of this group) have the same substrate, namely, a scissile bond in polypeptide chains. All of them have the same catalytic triad (His57, Asp102, Ser195, numbering after chymotrypsin) which is responsible for cleaving the peptide chain. Different members of this family cleave polypeptide chains preferentially at sites adjacent to specific amino acid residues. The structural basis for this preference lies in the shape of the specificity pocket (S1). Three residues, B189, B218, and B226, influence these preferences. For example chymotrypsin prefers the aromatic chain in this site, while trypsin favors positively charged amino acids, and uPA selects arginine. Other positions S2, S3, S4 or S1', S2' are involved in substrate recognition also, and molecules binding to them will inhibit uPA (10).

Most of the known PA inhibitors are non-specific in their inhibitory activity of tPA and uPA. Based on X-ray structure analysis and molecular modeling it seems that these inhibitors are mainly inserted into the specificity pocket (B187-B197; B212-B229) of uPA and tPA and block recognition site preventing binding of PAs to their substrate plasmin. This is the case of inhibition by small molecules such as benzamidine, p-benzamidine, and others (11-13).

Reduction of uPA activity in cancer cells has been traditionally associated with diminished invasion and metastasis. However, it has been shown recently that inhibitors of uPA could reduce tumor size also. Billstrom *et al.* (14) showed that p-aminobenzamidine, a competitive inhibitor of uPA, caused dose-dependent inhibition of uPA activity and decreased tumor-growth in DU-145 (human prostate cancer cells) inoculated SCID mice, when compared with non-treated animals. Amiloride, another uPA inhibitor, reduces tumor growth and decreases the proliferation of the tumor cells in the hepatomas and intestinal carcinomas (14).

Traditional thought holds that reduction of the proteolytic activity will reduce invasion and metastasis of cancer cells (3, 7, 8). In this way uPA inhibitors would have an important but somewhat, limited application in therapy, since in most cases, at the time of diagnosis metastatic micro foci are already formed. Far more interesting is the ability of uPA inhibitors to reduce tumor growth. Binding of proteolytically inactive ligand to uPA receptor, reduces amount of uPA on the surface of capillary endothelial cells and, by limiting availability of nutrients and oxygen, reduces tumor growth (10, 15, 16). Our studies have shown that uPA inhibitors reduce angiogenesis also in endothelial cells model, chick embryo model and in animals (16, 17).

It is imperative to search for novel selective inhibitors of uPA to be used in anti-cancer therapy. Novel drug candidate is checked on its potency on at least two different animal models, before it can advance to human phase of the research. Usually negative result on animal phase disqualifies drug candidate. Therefore, it is

very important to ask the question, if small chemical will inhibit uPA of different species with the same or similar potency. Using DNA sequences and known structure of uPA we have modeled 3D structures of several uPAs for different species including mouse, rat, and monkey proteins. As expected catalytic triad (B57, B102, B195) and specificity pocket (B187-B197, B212-B229) were highly conserved in all cases. These are regions responsible for proteolytic activity and recognition of the substrate. However, significant differences were observed in different region (loop B93-B101) that was identified by us as binding site of amiloride to the tissue (tPA) plasminogen activator (13). Amiloride is a specific inhibitor of uPA, but does not inhibit tPA, despite the fact that tPA shares the same function of activating plasminogen, and it is structurally similar to uPA. tPA attracts amiloride into a region different than the active site. This might be an indication that sequential and structural (topology) similarities in the active site and specificity pocket might be overruled by differences in recognition of inhibitor. To check this hypothesis, we have determined (by forcefield calculations) most probable structure for uPAs from different animals. Predicted position of amiloride depends on species and in some cases was located as expected in the specificity pocket, but in the others it was found close to the loop B93-B101. Placement of the inhibitor in this location might weaken or even prevent inhibition of uPA at all. In such case eliminating a drug based solely on animal study, without careful structural analysis, could lead to the elimination of a potential drug for humans.

Materials and Methods

DNA sequences. DNA sequences of uPA were obtained from <http://ca.expasy.org>, entries: human - P00749, yellow baboon - P16227, mouse - P06869, rat - P29598, chicken - P15120.

Obtaining the Starting Structure. All molecular modeling, and structure visualization were done on the SGI workstation, using *InsightII* program package from SGI. Atomic coordinates were retrieved from Protein Data Bank uPA - entry 1LMW (18), tPA - entry 1RTF (19). Hydrogen atoms were added and appropriate charges assigned throughout the studied molecules assuming physiological pH of 7.4. The partial and formal charges were assigned accordingly to the extensible systemic force field (esff) (10, 13, 20).

Homology protein structure modeling. In case when the 3D protein structure is not determined by X-ray crystallography or NMR, a 3D model of a given sequence can be calculated by comparative modeling. A protein sequence with at least 40% homology to a known structure can be modeled automatically with accuracy approaching that of a low-resolution X-ray structure. We have used the known structure of uPA as a template for all other uPAs in *Modeler* module of *InsightII* computer program. The sequential homology between human and animal uPA followed by number of amino acids and *rmsd* (Å) of C α -backbone were as follow: baboon 93.5% (0.38), mouse 71.0% (0.86), rat 50.0% (5.97 – this high number results from

extensive fragments having quite different folding) and chicken 50.2% (0.38).

Ligand design module - Ludi method for *de novo* design of ligands for proteins (*i. e.* enzyme inhibitors) is a useful method for screening a large number of compounds. This program analyzes a geometrical fit of given chemicals into the binding site and calculates other determinants of good binding such as hydrogen bonds, lipophilic interactions, ionic interactions, and acyclic interactions. Ludi scoring functions statistically evaluates the fit of all potential ligands.

$$\text{Ludi Score} = -73.33 \text{mol/kcal } \Delta G$$

where: $\Delta G = \Delta G_o + \Delta G_{hb}f(\Delta R)f(\Delta\alpha) + \Delta G_{ion}f(\Delta R)f(\Delta\alpha) + \Delta G_{lipo}A_{lipo} + \Delta G_{rot}NR \Delta G$; ΔG_o represents the contribution to the binding energy that does not directly depend on any specific interactions with the receptor (*i. e.* the contribution to binding energy due to loss of transitional and rotational entropy of the fragment), ΔG_{hb} and ΔG_{ion} represent the contribution from an ideal hydrogen bond and unperturbed ionic interactions, respectively, ΔG_{lipo} represents the contribution from lipophilic interactions which is proportional to the lipophilic surface A_{lipo} , ΔG_{rot} represents the contribution due to freezing of internal degrees of freedom in the fragment, NR is the number of acyclic bonds, ΔR is the deviation of the hydrogen bond length from the ideal value 1.9 Å, $\Delta\alpha$ is the deviation of the hydrogen bond angle from ideal value 180°. In general a higher Ludi score (0-1000 in range) represents a higher affinity and stronger binding of a ligand to the receptor.

In addition the Ludi Score could be related to a dissociation constant K_i .

$$\text{Ludi Score} = -100 \log K_i$$

Grasp visualization. Grasp is a computer program that visualize macromolecules surfaces and electrostatics. The program contains algorithms for the construction of rendered molecular surfaces, for solving the Poisson-Boltzmann equation and can be color-coded by electrostatic potential derived from its internal Poisson-Boltzmann solver. This permits a description of the electrostatic field generated by charges within a molecule such that the difference in dielectric constant between water (dielectric = 80) and the molecule (dielectric = 4), and also the influence of mobile ions (salt), are taken into account (21).

Results and Discussion

Computational methods predicting spatial interactions of protein/ligand complexes are rather successful. However, theoretical calculation of the affinity between protein and its inhibitors is considered less celebratory. Therefore, to assess an ability of *InsightII* programs to predict affinity, we have analyzed 147 protein/ligand structures with known affinity (22), and calculated their theoretical affinity using *Ludi* method for comparison. *Ludi* calculations are designed for non-binding protein-ligand complexes. However, some proteins bind its ligands forming chemical bonds

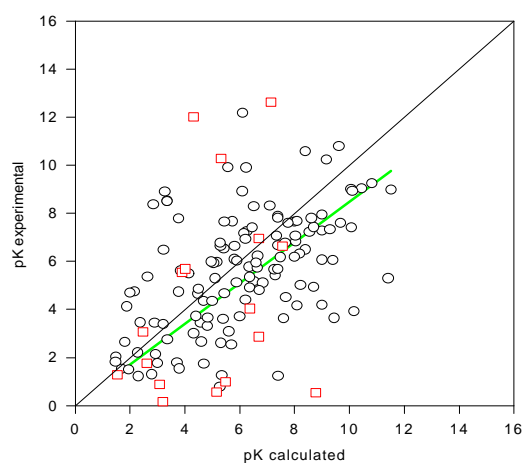


Fig 1. The correlation between the experimental and calculated pK values of 147 protein-ligand complexes. The correlation between the experimental and calculated pK values of the tested proteins is indicated by green line.

and these are shown on Fig. 1 and in Table 1 in red color. Our comparative study indicates that, in general *Ludi* method is slightly underestimating affinity of ligands, as it is shown on Fig. 1 by the green line (best fit). Affinity of the majority of analyzed ligand/protein complexes (68.5%) were within ± 2.0 pK, 81.1% within ± 3.0 pK. Also 60.6% of protein/ligands *Ludi* calculated affinities were within $\pm 30\%$ error of experimental value of pK. In $\pm 40\%$ region were 68.5% of analyzed proteins, when $\pm 50\%$ covered 84.3% of all complexes. All data above are for non-binding complexes. It must be noted that structure of these proteins was determined with different resolution and in some cases slight angular or linear movement of inhibitor or amino acid could easily effect and change value of *Ludi* calculated affinity (Table 1).

In a previous study (13) we have shown that uPA and, functionally and structurally similar, tPA bind amiloride in different regions of their molecules. Amiloride binds to uPA in the specificity pocket, while tPA binds it in the proximity of loop B93-B101, that is $\sim 15\text{\AA}$ distant (from B192 to B96) from the specificity pocket. Such position will not interfere with binding of tPA substrates and experimental data show that amiloride inhibits uPA but not tPA. Total charge of this loop in case of tPA was -5 but only -2 in case of uPA. By total charges we assume a sum of positively and negatively charged side chains of the amino acids. Probably this difference in electronegativity is responsible for differences in binding of positively charged amiloride to uPA and tPA. We have hypothesized that this loop could also be involved in binding of amiloride to uPAs of different species. Indeed, as it is shown on Table 2 total charge varies depending on species. It is interesting that distant species such as human and mice bind amiloride into the specificity pocket and have the most similar total charge in this loop, despite strong variation in amino acid composition in that particular region. When the total charge in that region raises amiloride tends to bind into the loop outside of active site (Fig 2). We observe, that the local electronegativity rather than sequential homology, seem to be that influential factor effecting positioning of the inhibitor. For example, baboon and human are the most similar topologically and differ by only

Table 1. Comparison of experimental (22) and *Ludi* calculated pKs.

Protein	pK	pK by Ludi	Abs[pK-Ludi]	Protein	pK	pK by Ludi	Abs[pK-Ludi]		
1.	2XIM	2.28	2.20	0.08	66.	2PK4	4.32	3.00	1.32
2.	3TMN	5.90	6.02	0.12	67.	1NNB	5.30	6.64	1.34
3.	1MCB	4.48	4.65	0.17	68.	2LDB	4.15	5.49	1.34
4.	6TIM	3.21	3.38	0.17	69.	1ABE	6.52	5.16	1.36
5.	6APR	7.77	7.59	0.18	70.	1HVJ	10.45	9.03	1.42
6.	1TNI	1.70	1.52	0.18	71.	1HBV	6.37	4.91	1.46
7.	1MDQ	5.10	5.29	0.19	72.	5ICD	5.29	6.77	1.48
8.	1SNC	6.70	6.95	0.25	73.	5ACN	2.80	1.29	1.51
9.	4XIA	1.54	1.29	0.25	74.	1FBP	4.82	3.30	1.52
10.	1PHH	7.35	7.06	0.29	75.	1EBG	10.82	9.25	1.57
11.	1PPM	5.80	6.09	0.29	76.	2CGR	7.27	5.66	1.61
12.	1GST	4.68	4.35	0.33	77.	2CTC	3.89	5.54	1.65
13.	1XLI	1.48	1.81	0.33	78.	3CPA	4.00	5.69	1.69
14.	1APW	8.00	7.64	0.36	79.	1APV	9.00	7.28	1.72
15.	3PTB	4.50	4.86	0.36	80.	2GBP	7.40	5.68	1.72
16.	1DRF	7.40	7.80	0.40	81.	1BAB	6.85	5.10	1.75
17.	1HTF	8.09	7.68	0.41	82.	2AK3	3.86	5.61	1.75
18.	1CPS	6.66	6.22	0.44	83.	2DRI	6.52	8.29	1.77
19.	1DHF	7.40	7.87	0.47	84.	7TIM	5.40	3.59	1.81
20.	1TNJ	1.96	1.49	0.47	85.	2R04	6.22	4.40	1.82
21.	1TNK	1.49	2.03	0.54	86.	7CAT	8.00	6.18	1.82
22.	1DWB	2.90	3.44	0.54	87.	1DWD	8.18	6.32	1.86
23.	1CBX	6.35	5.77	0.58	88.	1HSL	7.30	5.40	1.90
24.	7TNL	2.47	3.07	0.60	89.	1AAQ	8.40	6.49	1.91
25.	1TNH	3.37	2.75	0.62	90.	1DIH	5.74	7.66	1.92
26.	8ABP	6.60	5.95	0.65	91.	1RBP	6.72	4.79	1.93
27.	3GAP	5.00	4.34	0.66	92.	4TLN	3.72	1.78	1.94
28.	1ULB	4.40	3.72	0.68	93.	2PHH	4.60	2.65	1.95
29.	1PPH	6.22	6.92	0.70	94.	2FX2	9.30	7.33	1.97
30.	1DWC	7.41	6.66	0.75	95.	1HTG	9.68	7.59	2.09
31.	2TMN	5.89	5.11	0.78	96.	1ADB	8.40	10.57	2.17
32.	2IFB	5.44	4.66	0.78	97.	1LGR	3.07	0.88	2.19
33.	1RNT	5.18	5.97	0.79	98.	1LDM	5.44	7.65	2.21
34.	1TNG	2.93	2.14	0.79	99.	1TNL	1.88	4.12	2.24
35.	1BRA	1.82	2.63	0.81	100.	5ENL	3.80	1.53	2.27
36.	1APB	5.82	6.64	0.82	101.	1FBF	6.00	3.70	2.30
37.	4DFR	8.62	7.79	0.83	102.	5TLN	6.37	4.04	2.33
38.	5XIA	2.60	1.76	0.84	103.	4TS1	5.61	3.08	2.53
39.	6TMN	5.05	5.93	0.88	104.	6CPA	11.52	8.98	2.54
40.	1PPK	7.66	6.76	0.90	105.	4TIM	2.16	4.75	2.59
41.	1TLP	7.56	6.64	0.92	106.	1HVS	10.08	7.40	2.68
42.	5ABP	6.64	5.72	0.92	107.	5CNA	2.00	4.70	2.70
43.	7ABP	6.46	7.41	0.95	108.	1MFE	5.31	2.60	2.71
44.	1MCJ	3.78	4.73	0.95	109.	3CSC	2.64	5.36	2.72
45.	5TMN	8.04	7.07	0.97	110.	7DFR	6.10	8.91	2.81
46.	1FBC	6.26	7.25	0.99	111.	1MNC	9.00	6.06	2.94
47.	1PPC	6.16	7.17	1.01	112.	2MCP	4.70	1.73	2.97
48.	6ABP	6.36	5.34	1.02	113.	3PGM	3.19	0.16	3.03
49.	7DFR	4.96	5.98	1.02	114.	1PGP	5.70	2.53	3.17
50.	1HVL	9.00	7.94	1.06	115.	1DBJ	7.68	4.50	3.18
51.	1HVI	10.07	9.01	1.06	116.	1ETS	8.22	5.00	3.22
52.	4PHV	9.17	10.24	1.07	117.	4MDH	3.23	6.48	3.25
53.	6RNT	2.37	3.45	1.08	118.	1APT	9.40	6.04	3.36
54.	5TIM	2.30	1.21	1.09	119.	1RUS	3.08	-0.49	3.57
55.	1ABF	5.42	6.53	1.11	120.	1TMT	6.24	9.90	3.66
56.	1ADF	4.58	3.43	1.15	121.	2DBL	8.70	4.94	3.76
57.	1MCS	4.84	3.66	1.18	122.	2SNS	6.70	2.87	3.83
58.	7HVP	9.62	10.8	1.18	123.	1DBK	8.09	4.16	3.93
59.	1HVK	10.11	8.92	1.19	124.	7EST	7.60	3.62	3.98
60.	1CSC	7.10	8.31	1.21	125.	2RNT	3.78	7.77	3.99
61.	4FAB	8.05	6.82	1.23	126.	1THA	5.35	1.26	4.09
62.	6ENL	3.00	1.76	1.24	127.	5LDH	2.82	-1.38	4.20
63.	1RNE	8.70	7.42	1.28	128.	1DR1	5.57	9.92	4.35
64.	1APU	7.49	6.17	1.32	129.	4CLA	5.47	0.99	4.48
65.	1PPL	8.55	7.23	1.32	130.	1CLA	5.28	0.77	4.51
					131.	1MCF	5.15	0.57	4.58

Protein	pK	pK by Ludi	Abs[pK-Ludi]	
132. 1DDB		9.00	4.18	4.82
133. 5P21		5.32	10.28	4.96
134. 2PHH		3.36	8.49	5.13
135. 2CSC		3.36	8.51	5.15
136. 5SGA		2.85	8.37	5.52
137. 4SGA		3.27	8.90	5.63
138. 1DBM		9.44	3.64	5.80
139. 1MCH		5.15	-0.76	5.91
140. 4HVP		6.11	12.17	6.06
141. 1LYB		11.42	5.29	6.13
142. 1ETR		7.41	1.22	6.19
143. 4TMN		10.17	3.92	6.25
144. 4GR1		2.20	-4.31	6.51
145. 7ACN		4.31	12.01	7.70
146. 1TMN		7.47	-0.24	7.71
147. 1FKF		8.77	0.53	8.24

Table 3. Calculated pK for uPA of different species.

Human uPA	5.24
Baboon uPA	5.13
Mouse uPA	6.31
Rat uPA	2.31
Chicken uPA #1	1.74
Chicken uPA #2	4.60

one amino acid in selected region, but bind amiloride in a different fashion (Fig 2). The differences in surface charges of loop B93-B101 are well visible as red (negative) and blue (positive) areas of protein surfaces on Fig 3. Loop B93-B101 is negatively charged in mouse uPA, but this charge is canceled by positive

charge of arginine. Consequently amiloride binds into specificity pocket. It is noticeable that the orientation of the inhibitor is different between mouse and human uPA (Cl, O, etc), but the overall positioning of the flat moiety is very similar (Fig 2). When negative charge in this region reaches higher values amiloride binds to or in the proximity of loop B93-B101. This is especially expressive in case of human uPA and human tPA where region of loop B93-B101 is extensively negatively charged (red color on Fig 3). Spatial positioning of amiloride within uPA molecules is different between uPAs of different species, and definitely inactivates uPA molecules of human and mouse. In case of other molecules inhibition is less obvious, but still possible, since amiloride partially shields catalytic triad of uPA. However, in rat uPA amiloride is closer to the B93-B101 loop freeing more space in the catalytic triad area. Indeed some data from experiments on the animals indicate that amiloride is less effective as an anti-cancer drug in rats than in other animals (10, 17, 23-27).

Calculated pK = 5.24 for human uPA shows remarkable similarity to that determined by Vassalli in his experimental work and reported as pK = 5.15 (28, 29). There are no detailed data on amiloride/uPA complexes of other species. Nevertheless, experiments show that amiloride is effective anti-cancer agent in mouse, while it is less effective in rats. Also, inhibition of angiogenesis in chick embryo model requires rather sizeable amount of amiloride. Anti-cancer activity as well as inhibition of angiogenesis by amiloride is attributed to its ability to inhibit uPA. This is well in line with calculated affinity and position of amiloride in uPA molecules (Table 3).

In conclusion amiloride binds to uPA of different species with different affinity and in different place of uPA molecules. Amiloride therefore could inhibit uPA of some species in concentration much higher than in other cases, and that will be considered therapeutically undesirable. Rejection of the novel uPA inhibitors based solely on animal tests without careful structural analysis might lead to a lost of valuable anti-cancer drug for humans.

Table 2. Amino acid sequence in proximity of loops B93-B101 in different species. Bold numbers on the right indicate net electrostatic charge of that region.

Human uPA	Leu His Lys+ Asp- Tyr Ser Ala Asp- Thr Leu Ala His His Asn Asp- Ile -2
Baboon uPA	Leu His Glu- Asp- Tyr Ser Ala Asp- Thr Leu Ala His His Asn Asp- Ile -4
Mouse uPA	Leu His Glu- Tyr Tyr Arg+Glu-Asp- Ser Leu Ala Tyr His Asn Asp- Ile -3
Rat uPA	Leu His Glu- Asp- Phe Ser Asp-Glu- Thr Leu Ala Phe His Asn Asp- Ile -5
Chicken uPA	Ser His Pro Asp- Phe Thr Asp-His Thr Gly Gly Asn Asp-Asn Asp- Ile -4
Human tPA	Val His Lys+ Glu- Phe Asp-Asp-Asp- Thr - - Tyr Asp-Asn Asp- Ile -5

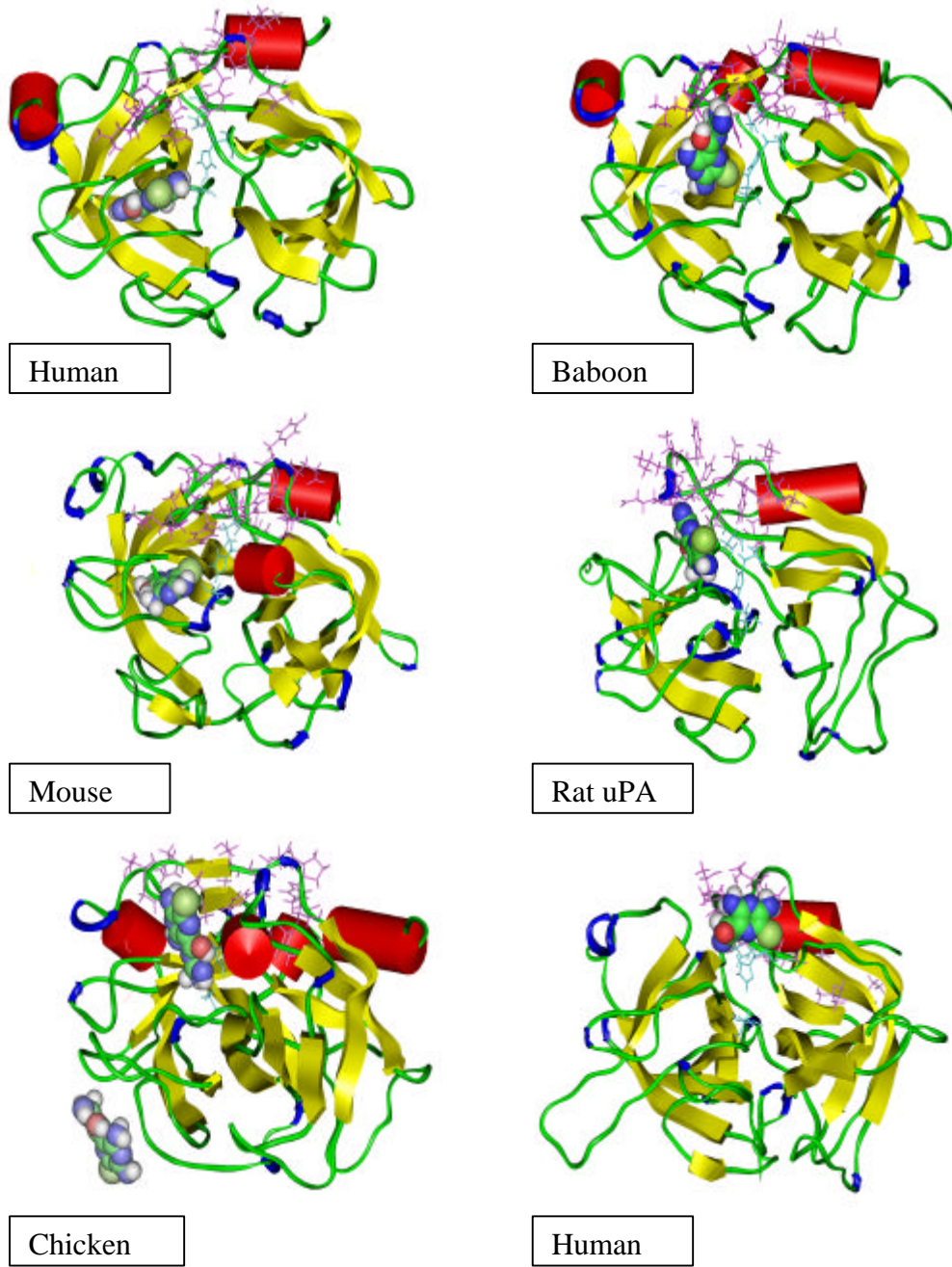


Fig 2. Ribbon models of plasminogen activators from different species. Helices are shown in red color, sheets in yellow, turns in blue and random coils are in green. Amino acids of Loops B93-B101 are shown as sticks in magenta when amino acids of specificity pockets are shown in light-blue.

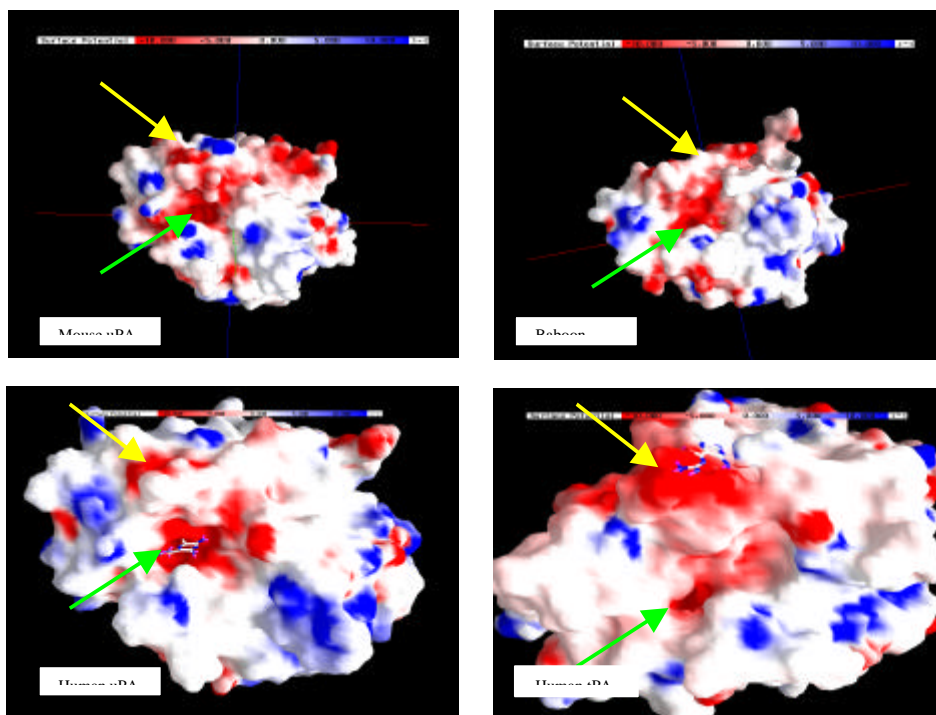


Fig 3. Grasp color-coded electrostatic potential of selected surfaces of plasminogen activators. Green arrows indicate specificity pocket, yellow loop B93-B101.

Acknowledgments

This work was supported in part by grants from: American Diagnostica Inc., Greenwich, CT., and Ohio Board of Regents

References

1. Conese M and Blasi F, The urokinase/urokinase-receptor system and cancer invasion. *Baillieres Clin Haematol.* 8(2): 365-389, 1995.
2. Festuccia C, Vincentini C, di Pasquale AB, *et al.*, Plasminogen activator activities in short-term tissue cultures of benign prostatic hyperplasia and prostatic carcinoma. *Oncol Res.* 7(3-4): 131-138, 1995.
3. Jankun J, Maher VM and McCormick JJ, Malignant transformation of human fibroblasts correlates with increased activity of receptor-bound plasminogen activator. *Cancer Res.* 51(4): 1221-1226, 1991.
4. Andreasen PA, Egelund R and Petersen HH, The plasminogen activation system in tumor growth, invasion, and metastasis. *Cell Mol Life Sci.* 57(1): 25-40, 2000.
5. Achbarou A, Kaiser S, Tremblay G, *et al.*, Urokinase overproduction results in increased skeletal metastasis by prostate cancer cells in vivo. *Cancer Res.* 54(9): 2372-2377, 1994.
6. Wilson MJ and Sinha AA, Plasminogen activator and metalloprotease activities of Du-145, PC-3, and 1-LN-PC-3-1A human prostate tumors grown in nude mice: correlation with tumor invasive behavior. *Cell Mol Biol Res.* 39(8): 751-760, 1993.
7. Jankun J, Merrick HW and Goldblatt PJ, Expression and localization of elements of the plasminogen activation system in benign breast disease and breast cancers. *J Cell Biochem.* 53(2): 135-144, 1993.
8. Ossowski L, In vivo invasion of modified chorioallantoic membrane by tumor cells: the role of cell surface-bound urokinase. *J Cell Biol.* 107(6 Pt 1): 2437-2445, 1988.
9. Ossowski L, Aguirre Ghiso J, Liu D, *et al.*, The role of plasminogen activator receptor in cancer invasion and dormancy. *Medicina (B Aires).* 59(5(Pt 2)): 547-552, 1999.
10. Jankun J, Keck RW, Skrzypczak-Jankun E, *et al.*, Inhibitors of urokinase reduce size of prostate cancer xenografts in severe combined immunodeficient mice. *Cancer Res.* 57(4): 559-563, 1997.
11. Goodson RJ, Doyle MV, Kaufman SE, *et al.*, High-affinity urokinase receptor antagonists identified with bacteriophage peptide display. *Proc Natl Acad Sci U S A.* 91(15): 7129-7133, 1994.
12. Zeslowska E, Schweinitz A, Karcher A, *et al.*, Crystals of the urokinase type plasminogen activator variant beta(c)-uPAin complex with small molecule inhibitors open the way towards structure-based drug design. *J Mol Biol.* 301(2): 465-475, 2000.
13. Jankun J and Skrzypczak-Jankun E, Molecular basis of specific inhibition of urokinase plasminogen activator by amiloride. *Cancer Biochem Biophys.* 17(1-2): 109-123, 1999.
14. Billstrom A, Hartley-Asp B, Lecander I, *et al.*, The urokinase inhibitor p-aminobenzamidine inhibits growth of a human prostate tumor in SCID mice. *Int J Cancer.* 61(4): 542-547, 1995.
15. Pepper MS, Sappino AP, Stocklin R, *et al.*, Upregulation of urokinase receptor expression on migrating endothelial cells. *J Cell Biol.* 122(3): 673-684, 1993.
16. Stefansson S, Petitclerc E, Wong MK, *et al.*, Inhibition of angiogenesis in vivo by plasminogen activator inhibitor-1. *J Biol Chem.* 276(11): 8135-8141, 2001.
17. Swierz R, Keck RW, Skrzypczak-Jankun E, *et al.*, Recombinant PAI-1 inhibits angiogenesis and reduces size of LNCaP prostate cancer xenografts in SCID mice. *Oncol Rep.* 8(3): 463-470, 2001.
18. Spraggon G, Phillips C, Nowak UK, *et al.*, The crystal structure of the catalytic domain of human urokinase-type plasminogen activator. *Structure.* 3(7): 681-691, 1995.
19. Lamba D, Bauer M, Huber R, *et al.*, The 2.3 Å crystal structure of the catalytic domain of recombinant two-chain human tissue-type plasminogen activator. *J Mol Biol.* 258(1): 117-135, 1996.
20. Jankun J, Selman SH, Swierz R, *et al.*, Why drinking green tea could prevent cancer. *Nature.* 387(6633): 561, 1997.
21. Nicholls A, Sharp KA and Honig B, Protein folding and association: insights from the interfacial and thermodynamic properties of hydrocarbons. *Proteins.* 11(4): 281-296, 1991.
22. Wang R, Liu L TY, SCORE: A New Empirical Method for Estimating the Binding Affinity of a Protein-ligand Complex. *Journal of Molecular Modeling.* 4: 379-394, 1998.
23. Evans DM and Sloan-Stakleff KD, Maximum effect of urokinase plasminogen activator inhibitors in the control of invasion and metastasis of rat mammary cancer. *Invasion Metastasis.* 18(5-6): 252-260, 1998.
24. Evans DM, Sloan-Stakleff K, Arvan M, *et al.*, Time and dose dependency of the suppression of pulmonary metastases of rat mammary cancer by amiloride. *Clin Exp Metastasis.* 16(4): 353-357, 1998.
25. Ray P, Bhatti R, Gadarowski J, *et al.*, Inhibitory effect of amiloride on the urokinase plasminogen activators in prostatic cancer. *Tumour Biol.* 19(1): 60-64, 1998.
26. Kellen JA, Mirakian A and Kolin A, Antimetastatic effect of amiloride in an animal tumour model. *Anticancer Res.* 8(6): 1373-1376, 1988.
27. Swierz R, Skrzypczak-Jankun E, Merrell MM, *et al.*, Angiostatic activity of synthetic inhibitors of urokinase type plasminogen activator. *Oncol Rep.* 6(3): 523-526, 1999.
28. Pepper MS, Vassalli JD, Montesano R, *et al.*, Urokinase-type plasminogen activator is induced in migrating capillary endothelial cells. *J Cell Biol.* 105(6 Pt 1): 2535-2541, 1987.
29. Vassalli JD and Belin D, Amiloride selectively inhibits the urokinase-type plasminogen activator. *FEBS Lett.* 214(1): 187-191, 1987.